A luminescent europium hairpin for DNA photosensing in the visible, based on trimetallic bis-intercalators

Scarpantonio, Luca; Cotton, Simon A.; Del Giorgio, Elena; Mccallum, M.; Hannon, Mike; Pikramenou, Zoe

DOI:
10.1016/j.jinorgbio.2020.111119

Document Version
Peer reviewed version

Citation for published version (Harvard):
Scarpantonio, L, Cotton, SA, Del Giorgio, E, Mccallum, M, Hannon, M & Pikramenou, Z 2020, 'A luminescent europium hairpin for DNA photosensing in the visible, based on trimetallic bis-intercalators', *Journal of Inorganic Biochemistry*, vol. 209, 111119. https://doi.org/10.1016/j.jinorgbio.2020.111119

A luminescent europium hairpin for DNA photosensing in the visible, based on trimetallic bis-intercalators

L. Scarpantonio, S. A. Cotton, E. del Giorgio, M. McCallum,[&] M.J. Hannon and Z. Pikramenou*

School of Chemistry, University of Birmingham, Edgbaston, B15 2TT, UK

[&] Edinburgh Instruments Ltd. Livingston, EH54 7DQ, UK

e-mail: z.pikramenou@bham.ac.uk; https://orcid.org/0000-0002-6001-1380

Abstract

Luminescence monitoring of DNA intercalator complexes is important for assessing their localisation and targeting: We report herein a luminescent hetero-trimetallic complex with europium as a luminescent reporter and two attached platinum acetylide terpyridyl units as the DNA recognition units. The ligand, based on a bisamide derivative of diethylenetriaminepentaacetic acid functionalised with two ethynyl groups, provides a backbone to anchor two platinum terpyridyl units, Pt-tpy, leading to the hairpin-shaped heterometallic complex **1**. We also prepared a related mono-nuclear platinum complex **2** to compare its intercalation properties with **1**. Linear dichroism, UV-visible and melting experiments show the ability of both complexes to interact with calf thymus DNA, with linear dichroism confirming intercalation and demonstarting the expected greater DNA stiffening by the bis-intercalator **1**. Importantly, the tri-metallic complex **1** shows a three-fold enhancement in europium luminescence upon addition of calf thymus DNA; other mono-intercalator lanthanide designs have commonly shown a decrease in emission on binding. The ability of the complex to monitor DNA interactions gives the potential use as a luminescence switch in sensing experiments and highlights the design of heterometallic bis-intercalator complexes as an effective approach for DNA-responsive sensitisation of a lanthanide luminescence signal.

Keywords

Lanthanide, DNA intercalation, heterometallic complexes, luminescence, sensitisation

1. Introduction

Polymetallic nanostructures bring novel, distinct, recognition features to their interaction with nucleic acids, which govern the sensing function in diagnostic assays and their application in photodynamic therapy.[1-11] The effect of bis-intercalator units on the

structural changes to DNA is of particular interest because the tethering of the two intercalators affects the DNA-binding and this can also influence the biological activity.[12-20] We have previously introduced the bisamide of diethylene triamine pentaacetic acid (DTPA) as a scaffold for the attachment of platinum units to form DNA bis-intercalators [20] in order to introduce a luminescent lanthanide site "remote" from the intercalating unit. The DTPA bisamide ligand provides a versatile design for the formation of multinuclear complexes with selective substitution of the bisamide arms. [21-25] In our previous studies, platinum terpyridyl units. Pt-tpy (tpy = 2,2';6',2''-terpyridine), were attached *via* thiophenol moieties to the DTPA-bisamide but the presence of a thiophenol to terpyridyl charge transfer state in the visible region limited the luminescence properties of the complexes. In this manuscript we introduce an improved DTPA-bisamide scaffold with platinum acetylide chromophores which are popular photoactive units with luminescence signal sensitive to the environment.[26-35] Furthermore, the acetylide link provides a tool to shift the charge transfer band from the Pt to tpy* and/or the acetylide to tpy* away from the europium emission spectral region (Scheme 1).

Complex **1** includes three structural features: Pt-tpy as DNA recognition unit, a lanthanide lumophore encapsulated in the DTPA-(bisamide) core and a phenyl acetylide link that keeps the overall amide conformation in a rigid hairpin like structure with two intercalating units. Additionally, the acetylide link brings synthetic feasibility and allows tuning of photophysical properties of Pt-tpy. We also isolated a Pt-tpy acetylide complex **2** which is a model of the individual DNA recognition units of **1** and would act as a mono-intercalator to compare and contrast the recognition properties. The luminescence properties as well as the intercalation behaviour with calf thymus DNA (ctDNA) of both **1** and **2** are studied using luminescence and linear dichroism spectroscopic methods.

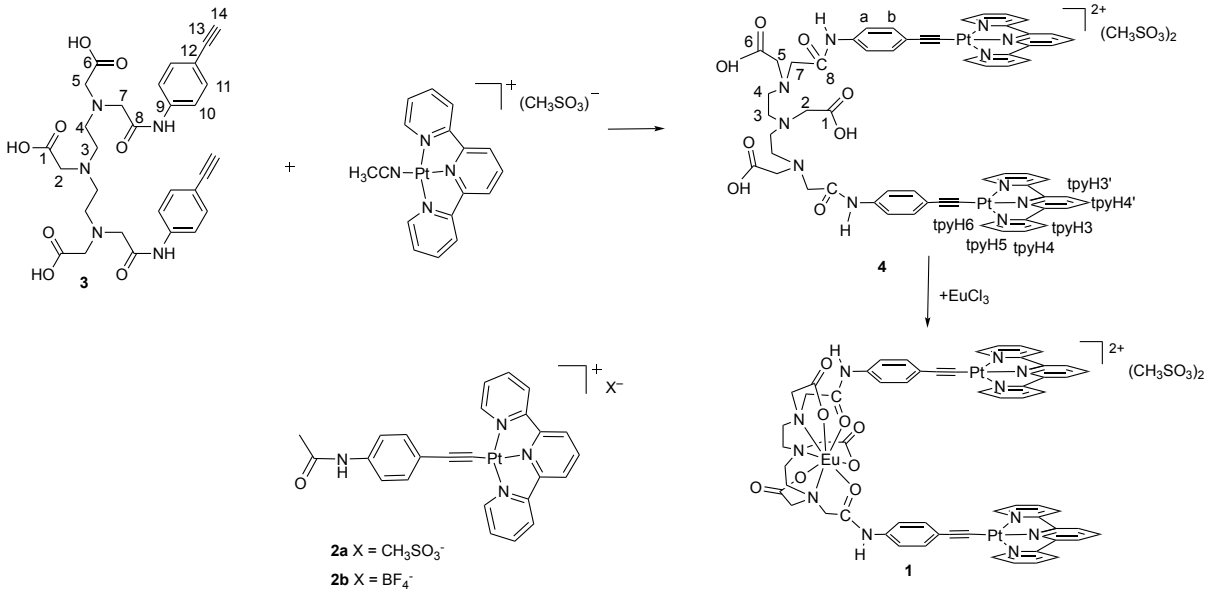

Scheme 1. Method for preparation of trimetallic complex **1** and structure of complex **2** prepared as a control comparison.

2.Materials and Methods

All solvents and chemicals were purchased from Sigma-Aldrich and were used without further purification. Deuterated solvents were purchased from Goss Scientific or Sigma-Aldrich and used as received. HPLC-grade solvents were used in photophysical studies. Water was deionized by use of an Elga Option 3 water purifier. $[Pt(tpy)(CH_3CN)](CH_3SO_3)_2$ and the N-(4-ethynylphenyl) acetamide were synthesized following previously reported procedures,[36-39] while all ligand and complex synthetic procedures were carried out under nitrogen with degassed anhydrous solvents. ^{1}H and ^{13}C-$\{^{1}H\}$ NMR spectra were obtained on Bruker AC 300, AV 300, AMX 400, AV 400 or DRX 500 spectrometers. Electrospray mass spectra were recorded on a Micromass LC-TOF machine and matrix-assisted laser desorption ionization (MALDI) mass spectra were recorded on a Brüker Biflex IV mass spectrometer. Elemental analyses were recorded on a Carlo Erba EA1110 simultaneous CHN elemental analyzer at the University of Birmingham.

Steady-state luminescence experiments were carried out on a Photon Technology Instruments fluorescence system equipped with a 75 W xenon arc lamp as the illumination source, single excitation and emission monochromators, the latter with grating blazed at 500 nm and a Hamamatsu R928 photomultiplier tube. Spectra were recorded by use of PTI Felix fluorescence analysis software. Luminescence lifetime data were recorded on an Edinburgh Instruments FLS1000-SS-stm using a PMT-900 (R928P

from Hamamatsu). Luminescence quantum yield was measured by an optically dilute relative method using $[Ru(2,2'\text{-bipyridyl})_3]Cl_2$ ($\Phi = 0.045$ in aerated H_2O) as a standard.

Calf-thymus ctDNA (highly polymerised) was purchased from Sigma-Aldrich and it was dissolved in water without any further purification. The concentration was determined spectroscopically using the molar extinction coefficients at the wavelength of maximum absorption: ctDNA $\lambda_{260} = 6600$ mol^{-1} dm^3 cm^{-1}. All DNA experiments were performed using a HEPES buffer (pH = 7), effective over a neutral pH range, with added sodium chloride.

Linear dichroism (LD) spectra were collected on a Jasco J-715 spectropolarimeter adapted for LD measurements. For flow linear dichroism experiments the samples were orientated in a radial couette flow cell, a small volume cylindrical quartz cell, with pathlength 1 mm, the centre of which was rotated by an electric motor during the course of the experiment. All LD spectra were recorded at 20 ˚C.

DNA melting studies were carried out using a Varian Cary 5000 UV-Vis-NIR spectrophotometer equipped with Cary temperature controller. Spectra were recorded using Cary WinUV software. Helix melting was monitored by following the absorption of the sample at 260 nm, as a function of temperature. The melting temperature (T_m) was determined from the first derivative of a plot of absorption versus temperature. The following parameters were used: 0.5 ˚C data interval and 0.5 ˚C/min rate.

3. Experimental

Synthesis

3. 4-Aminoethynylaniline (1.32 g, 11.2 mmol) was added to a stirring suspension of DTPA bis(anhydride) (1 g, 2.8 mmol) in triethylamine (10 cm^3). The solution was stirred under nitrogen for 24 h at room temperature. A cloudy pale yellow solution was obtained. The solvent was removed under *vacuo* at 40 ˚C and a yellow solid was obtained. The solid was treated with ethyl acetate and left stirring overnight at room temperature. A pale yellow precipitate was isolated by filtration and washed (2 × 25 cm^3) with ethyl acetate and (2 × 25 cm^3) diethyl ether. The crude ligand was re-dissolved in the minimum amount of water and the pH lowered to 3 via the dropwise addition of 0.1 M hydrochloric acid. The solution was refrigerated overnight and the resulting precipitate was collected by decanting. The off-white solid was then stirred vigorously in 25 cm^3 of ethylacetate to

afford an off-white powder. The powder was collected by filtration and washed with diethyl ether (2 × 20 cm^3) to yield 0.73 g (44 %).

^{1}H NMR (400 MHz, CD_3OD, 24 ºC) δ = 7.52 (d, 4H, H10), 7.23 (d, 4H, H11), 3.78 (s, 2H, H2), 3.49 (s, 4H, H5), 3.41 (s, 4H, H7), 3.35 (t, J = 5.7 Hz 4H, H4), 3.28 (s, 2H, H14), 3.12 (t, J = 5.7 Hz, 4H, H3); ^{13}C {^{1}H} NMR (100 MHz, CD_3OD with 5 % NaOD, 24 °C,TMS) δ = 173.4 (C1), 169.0 (C6), 168.0(C8), 137.3 (C9), 130.9 (C11), 118.6 (C10), 116.6 (C12), 81.7 (C13), 75.4 (C14), 64.3 (C5), 57.7 (C7), 55.0 (C2), 53.5 (C4), 52.9 (C3); IR (KBr): ν in cm^{-1} = 3277 (s), 2103(m), 1670 (s); MS/ES$^+$ = 590 [M]$^+$, 295.5 [M]$^{2+}$; UV-Vis (CH_3OH): λ_{max} in nm 270; Elemental Analysis calcd (%) for $C_{30}H_{33}N_5O_8$ 0.5(H_2O): C, 60.0; H, 5.7, N 11.7; found: C, 60.2; H, 6.1; N, 11.4.

2a Sodium methoxide (9.57 mg, 0.177 mmol) was added to a stirred solution of N-(4-ethynylphenyl)acetamide (28 mg, 0.177 mmol) in methanol under nitrogen. The resultant solution was stirred at room temperature for 30 min. [Pt(tpy)(CH_3CN)](CH_3SO_3)$_2$ (50 mg 0.088 mmol) was added to the reaction mixture which turned to a red solution and was brought to reflux for 2h. The solvent was removed and the deep red precipitate was dissolved in the minimum amount of water. By dropwise addition of acetonitrile a red precipitate **2a** was isolated by filtration and washed with 20 cm^3 of acetonitrile and 20 cm^3 of diethyl ether to give 41 mg (yield 68 %).

^{1}H NMR (300 MHz, D_2O, 24 ºC) δ = 8.50 - 7.20 (m, 9H), 2.49 (s, 3H), 2.29 (s, 3H); MS/ES$^+$: 586 [M- CH_3SO_3] $^+$; IR (KBr) ν in cm^{-1} = 3041 (m), 2115 (m), 1669 (s), 1583 (s), 1508 (s); UV-Vis (CH_3OH): λ_{max} in nm 470, 345, 330, 280, 255.

In a similar method as **2a**, compound **2b** was prepared by precipitation with a saturated methanolic solution of NH_4BF_4 as a fine deep red precipitate which was collected by filtration and washed with methanol (20 cm^3) and diethyl ether (20 cm^3) to obtain 39 mg of compound **2b** (yield 73 %).

^{1}H NMR (300 MHz, CD_3OD, 24 ºC) δ = 8.79 (d, J(Pt, H) = 46 Hz, J(H,H) = 5.6 Hz, H6), 8.30 - 8.14 (m, 4H, H4, H4'), 8.10 - 8.00 (m, 3H, H3', H3), 7.60 (dd, 2H, ^{3}J(H,H) = 8.1 Hz, 5.6 Hz, H5), 7.60 (d, 2H, J(H,H) = 8.5 Hz, Ar-Ha), 7.28 (d, 2H, J(H,H) = 8.5 Hz, Hb), 2.11 (3H, s, CH3); IR (KBr): ν in cm^{-1} = 3073 (m), 3040 (m), 2115 (m), 1669 (s), 1593 (s), 1508 (s), 1036 (s); MS (ES$^+$) m/z= 586 [M-(BF_4)] $^+$; UV-Vis (CH_3CN): λ_{max} in nm 470, 345, 330, 280, 255. Elemental Analysis calcd (%) for $C_{25}H_{19}N_4OPtBF_4H_2O$: C, 43.4; H, 3.1, N 8.1; found: C, 43.6; H, 2.8; N, 8.0.

4 Sodium methoxide (10 mg, 0.2 mmol) was added upon stirring to a solution of **3** (23 mg, 0.04 mmol) in methanol under a nitrogen atmosphere. The resulting solution was left stirring at room temperature for 30 min. [Pt(tpy)(CH_3CN)](CH_3SO_3)$_2$ (50 mg, 0.09 mmol)

was added to the reaction mixture which turned red colour and was heated under reflux for 2h at 80 ˚C. The solvent was removed and the deep red solid was dissolved in deionised water (10 cm^3). The pH was lowered to 3.0 by dropwise addition of methane sulfonic acid 0.1 M. The solvent was then reduced to approximately 2 ml and dropwise addition of acetonitrile afforded a red precipitate that was isolated by filtration and washed with acetonitrile (2x10 cm^3) and diethyl ether (20 cm^3) to give compound 38 mg of **4**, yield 58%. MS/MALDI: 1446.3 $[M -2(CH_3SO_3)+H]^+$; IR (KBr) ν in cm^{-1} = 3074 (m), 2109 (m), 1609 (s), 1601 (s), 1173 (s); UV-Vis (H_2O): λmax in nm 420, 280. ^1H NMR (300 MHz, D_2O, 5 % NaOD, CD_3OD, 24 ºC) δ in ppm: 8.7-8.2 (tpy-H6, tpy-H4, tpyH4'), 8.0-7.8(tpy H3, tpyH3'), 7.6-7.2 (H10, H11, tpy-H5), 3.75 (H2), 3.50 (H5), 3.40-2.40 (H7, H4, H3).

1. Compound **4** (50 mg 0.03 mmol) was dissolved in a minimum amount of deionised water and the pH was raised to 5.5 by the dropwise addition of tetrabutyl ammonium hydroxide (40 % w/w), followed by the addition $EuCl_3 \cdot 6H_2O$ (0.03 mmol). The solvent was then reduced and acetonitrile was added. The fine red precipitate was isolated by filtration and washed with acetonitrile (2 × 10 cm^3) and diethyl ether (2 × 20 cm^3) to give 19.3 mg of **1**, yield 65 %. MS /ES^+: 797.6 $[M -2(CH_3SO_3)]^{2+}$, MALDI: 1595.2 $[M -2(CH_3SO_3)]^+$; UV-Vis (H_2O): λ_{max} in nm 420, 280. Elemental Analysis calcd (%) for $C_{62}H_{56}N_{11}O_{14}EuPt_2S_28H_2O$: C, 38.6; H, 3.8, N 8.0; found: C, 38.4; H, 3.5; N, 8.4.

4. Results and discussion

4.1 Synthesis and characterisation

The complex **1** was prepared by a stepwise approach (Scheme 1). In order to assess the binding properties of **1** as a DNA intercalator, it was desirable to compare it with the mononuclear analogue complex, thus **2a**/**2b** were also synthesised and characterised.

The bis-acetylide DTPA derivative, **3**, was prepared from 4'-ethynylaniline and the bis(anhydride) of diethylene triamine pentaacetic acid (DTPA) following previous, related methodologies[40,41] to provide the acetylide reactive group[42] to coordinate to platinum. The ^1H-NMR spectrum shows the characteristic acetylide resonance H14 that appears as a singlet at 3.28 ppm. The ^{13}C-NMR spectrum of **3** shows 16 carbon resonances, and the terminal CH arising from the acetylide unit are displayed at 81.7 ppm. All assignments were facilitated by heteronuclear single quantum correlation, HSQC, analysis and agree with the previously reported ligand.[42]

We used a versatile platinum complex $[Pt(tpy)(CH_3CN)](CH_3SO_3)_2$ to attach to **3** in presence of sodium methoxide based on previous methods for such couplings. [36,37,43].

The resulting compound, **4**, had a characteristic red colour due to the charge transfer band that is present also in complex **2** (Supplementary Info) and was fully characterised by NMR and mass spectrometry. The DTPA backbone resonances agree with the pattern of compound **3,** while ^{1}H-^{1}H correlation spectroscopy (COSY) was employed to reveal the couplings of the overlapping protons in the aromatic region. The mass spectrum of the bimetallic complex shows a characteristic peak at m/z 1446.3 corresponding to [M - 2(CH_3SO_3)+H]$^{+}$. Upon complexation of **4** with europium the trimetallic complex **1** was isolated. Due to the paramagnetism of the europium, analysis was restricted to mass spectrometry and photophysical studies. MALDI and electrospray mass spectrometry show characteristic ion peaks of the trimetallic complex for the singly- and doubly-charged species (Figure 1 and theoretical patterns in Supplementary Info).

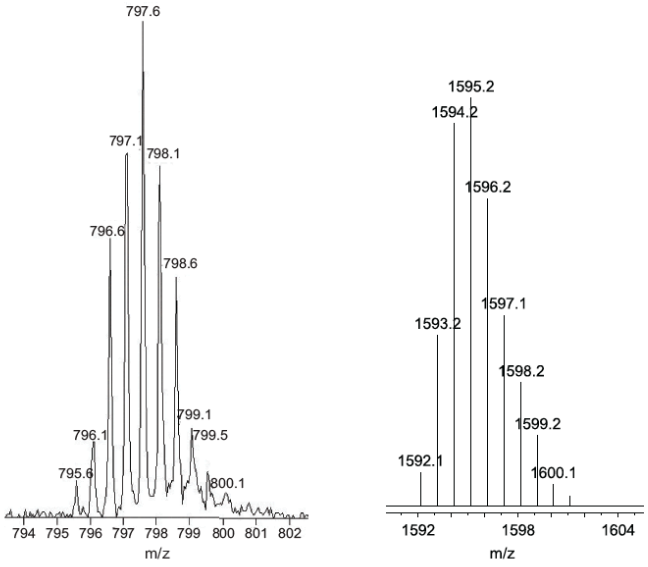

Figure 1. ES-MS(+) (a) and MALDI (b) spectra of **1** spectra corresponding to [M - 2(CH_3SO_3)]$^{2+}$ and single charged [M -2(CH_3SO_3)]$^{+}$ species, respectively.

The UV-vis absorption spectrum of **1** in methanol (Figure 2) is dominated by intense absorption bands in the UV region of the spectrum which are attributed to the $\pi \rightarrow \pi^*$ transitions and a characteristic broad band in the visible between 400 and 500 nm, which is attributed to a charge transfer band dominated by the metal to ligand charge transfer (MLCT) dπ(Pt)$\rightarrow \pi^*$(tpy) transition, with possible contribution from the ligand to ligand charge transfer (LLCT) π(PhC≡C) $\rightarrow \pi^*$(tpy) as also observed in related platinum complexes [33,29] and in the spectrum of complex **2b** (Supplementary Info). The molar

absorptivity of the charge transfer band in **1** is doubled in comparison to the value in **2b,** confirming the presence of the two platinum units. This band is blue-shifted in comparison with the LLCT observed in our previously reported trimetallic complex where the platinum centres are attached *via* thiophenolate links to the DTPA backbone.[2]

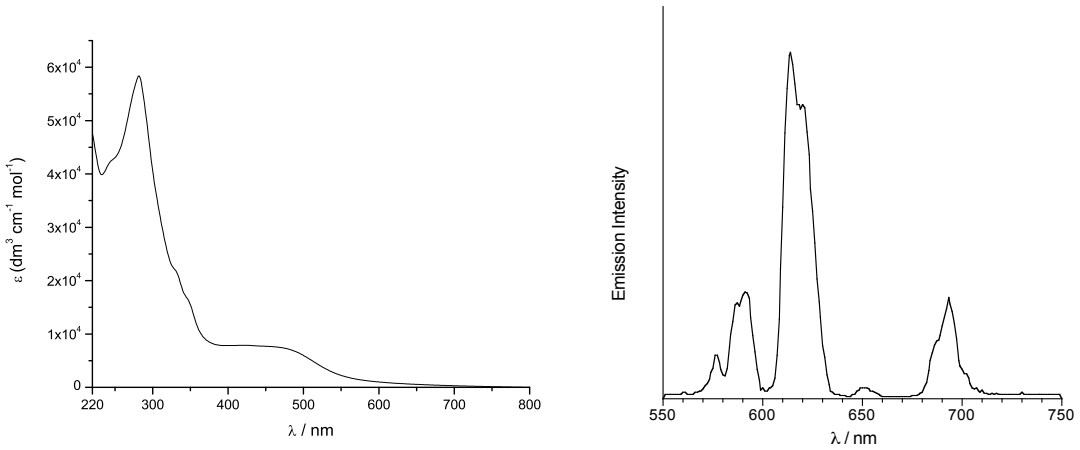

Figure 2. Absorption and emission (λ_{exc} = 280 nm) spectra of **1** in methanol.

Upon excitation at 280 nm, complex **1** displays the characteristic europium emission band due to luminescent transitions $^5D_0 \rightarrow {}^7F_J$ (J= 0, 1, 2, 3, 4) at 580, 590, 615, 650 and 695 nm respectively (Figure 2). Excitation at the 450 nm band did not lead to any europium or platinum-based emission even when the solution was degassed. This is also confirmed by the excitation spectra which show that the bands responsible for sensitisation of the emission are the π- π* based on the terpyridine or the phenyl acetylide chromophores (Supplementary Info). The mononuclear platinum complex **2b** displays luminescence at λ_{max} = 585 nm upon excitation of the charge transfer band (λ_{max}= 430 nm) (Supplementary Info) in acetonitrile solutions but only when deoxygenated with nitrogen. Previously reported photophysical studies for similar platinum acetylide complexes, have attributed this platinum-based emission to the ^{3}MLCT.[30,28]

The lack of sensitisation of europium emission by the charge transfer band may be due to the mixed character of the charge transfer and/or the poor electronic coupling with the europium centre, resulting in an inefficient energy transfer process by the exchange mechanism, or may imply the presence of an electron transfer quenching pathway. However, excitation at the tpy-based transitions at 330 and 345 nm leads to europium luminescence, which indicates that the terpyridine unit can sensitise the europium remotely and further away from the DTPA backbone. The complex displays a quantum yield of 0.4 % in methanol which is ten times higher than a corresponding europium complex with a simple thiophenol sensitiser.[23] Upon excitation at 300 nm the

luminescence lifetime of the complex in methanol was found to have a major long component of 656 μs and two minor components of 114 and 5 μs (relevant percentages, 72 %, 5 % and 23 %, respectively). The short components may indicate the possible presence of photoinduced electron transfer pathways from the charge transfer transitions.

4.2 DNA binding studies

To explore the DNA-binding of the agents we first monitored the effect on the UV-vis absorption spectroscopy of the Pt-tpy units on adding calf-thymus ctDNA (a polymeric genomic DNA) (Figure 3). Although the changes in the complex spectroscopy are small for both **1** and **2a** (Supplementary Info) they confirm interaction of both complexes with the DNA. They indicate that the complex does not undergo significant structural change on binding; small bathochromic shifts in the charge transfer bands (~470 nm) are consistent with the anticipated intercalative mode of binding.

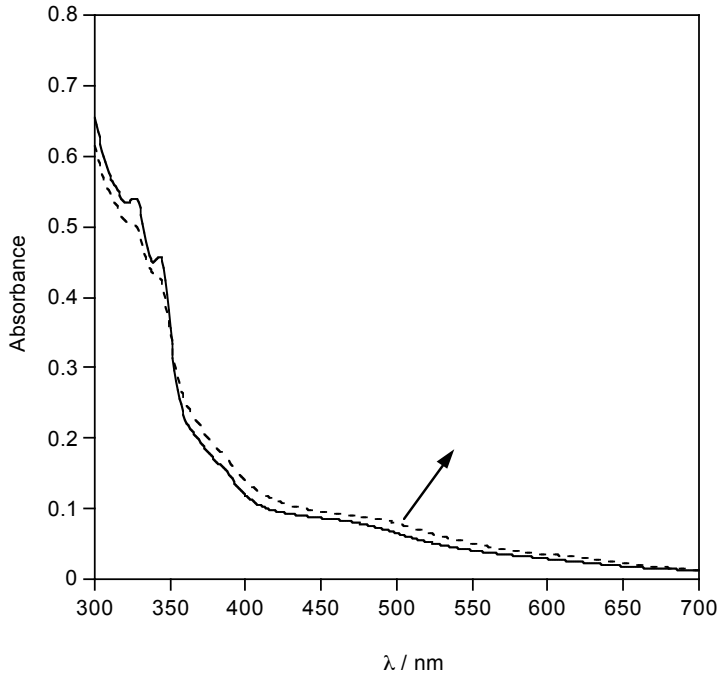

Figure 3. Absorption spectrum of **1** in absence (10 μM, solid line) and presence of ctDNA (ratio DNA:complex 4:1, dashed line) in 10 mM HEPES buffer and 10 mM of NaCl.

Complex **1** stabilises the DNA structure on binding, as evidenced by DNA melting studies (Figure 4, monitoring at 260nm). At a ratio of 20:1 DNA/complex we observed a ΔT_m of 10 ˚C, with further additions to reach a 4 : 1 ratio leading to smaller further increases (ΔT_m = 12 ˚C).

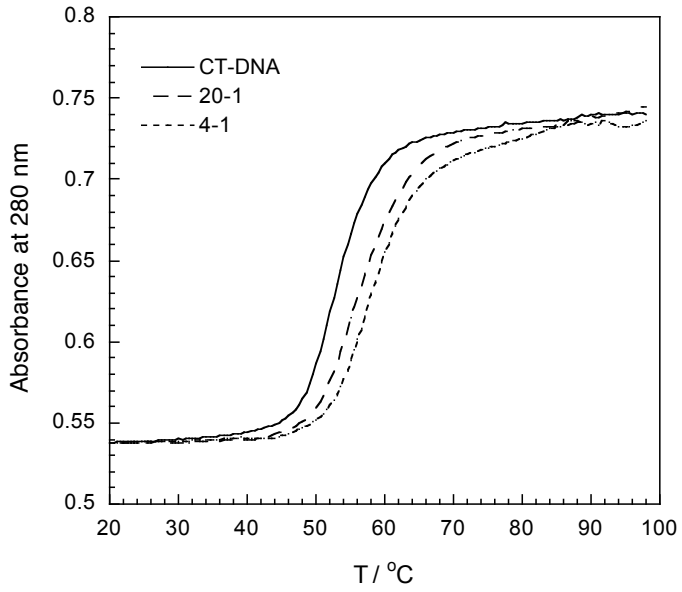

Figure 4. Melting curves of ctDNA (60 μM) in the presence of 1 (ratio 4:1, DNA:complex) in 10 mM HEPES buffer and 10 mM of NaCl.

To directly probe and confirm the potential intercalative binding mode we used flow linear dichroism (LD) spectroscopy.[44,45,2] Long polymeric ctDNA is orientated by viscous drag in a Couette cell, and its orientation assessed by the difference in absorption of light linearly polarised parallel and perpendicular to the orientation direction. B-DNA gives a negative LD signal at λ = 260 nm (arising from π–π* transitions) as its bases are almost perpendicular to the orientation axis of the DNA, with the magnitude of the LD signal reflecting the degree of DNA orientation. The LD signal of ctDNA decreases upon addition of both **1** and **2** as is typically observed when DNA stiffening is caused by the presence of intercalative agents (Figure 5 and Supplementary Info). Neither **1** nor **2** are of sufficient size to be oriented in such a flow when alone (and so give no signal). However on addition to DNA, induced linear dichroism (ILD) signals are observed in the spectroscopies of both **1** and **2**. These ILD bands at ~330 and ~450 nm are not only unambiguous confirmation of binding between these complexes and DNA, but they confirm that the complexes are binding not randomly but rather in specific orientation(s). The negative sign of these signals indicated that the Pt-tpy units lie orthogonal to the main B-DNA axis, parallel with the DNA bases. Taken together with the observation of DNA stiffening this is strong evidence that the mode is indeed the expected intercalative binding mode, as also seen in LD for a previous Pt(terpy)(alkyne) species.[29] It is notable that the stiffening and ILD effects are seen at much lower loading for **1** than **2** (for which high loading is needed) consistent with anticipated stronger binding afforded by the pair of Pt(tpy) units in **1**.

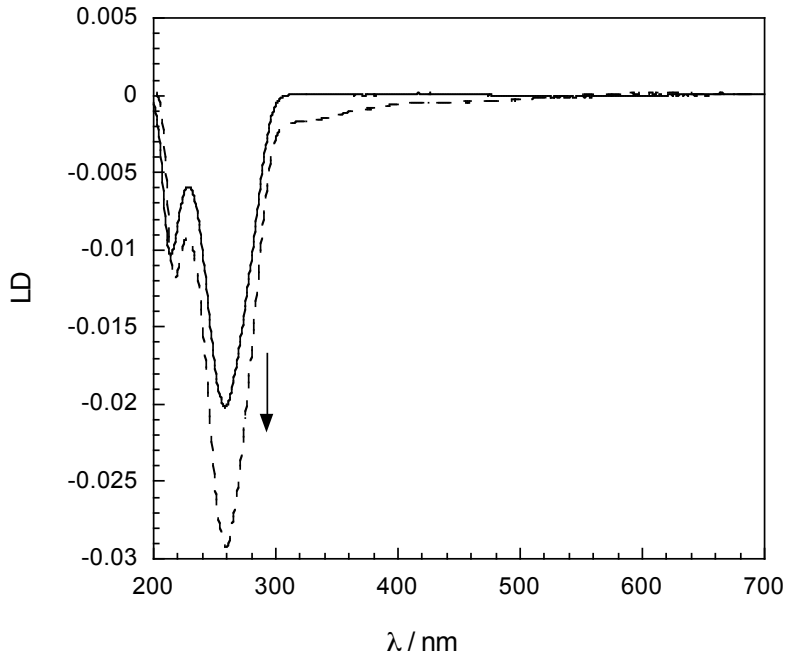

Figure 5. LD spectra of ctDNA (solid line) upon addition of **1** in a ratio (40:1) in 10mM HEPES buffer and 10 mM NaCl.

The emission spectra of **1** were recorded in the presence of increasing concentrations of ctDNA (Figure 6). An excitation wavelength at 300 nm was selected, where the tpy absorbs but there is least interference from DNA absorption, yet the excitation is still efficient for energy transfer to the lanthanide. Upon addition of aliquots of ctDNA to a solution of **1**, an increase of the europium signal was observed with a three-fold enhancement of the europium signal at the ratio of DNA:**1** of 4:1. The ratio of the 590 and 613 bands is unchanged upon intercalation, confirming that the europium coordination environment remains unchanged when the complex binds to DNA. It is well documented that the Pt-tpy unit is sensitive to variation of the solvent polarity.[28] Upon interaction with DNA, intercalation of the platinum units positions them in a hydrophobic environment, within the internal part of the DNA double helix. This is expected to lead to two effects. Firstly, the intercalation will sterically restrain conformational freedom of the complex and in particular the tpy moieties. Secondly, the tpy is now positioned in an electron rich environment and this will affect the LLCT contribution to the charge transfer band. Both of these effects will influence the energy transfer pathway to the lanthanide, and potentially reduce electron transfer quenching, leading to the observed increase in europium emission. We also investigated the possibility of using the characteristic charge transfer band of **1** to sensitise the europium luminescence upon addition of DNA. Upon

excitation of complex **1** at the charge transfer band at 450 nm in the presence of ctDNA, we did not observe any europium-based emission. Thus, the intercalation does not affect the sensitising properties of the charge transfer band for europium emission.

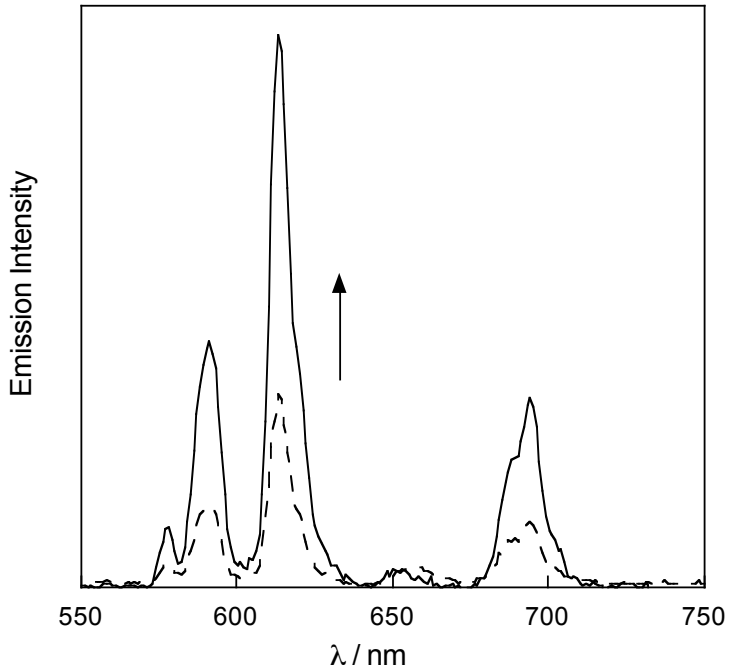

Figure 6. Emission spectra of **1** (dashed line) and in presence of ctDNA (solid line) in a ratio (1:4) in 10mM HEPES buffer and 10 mM NaCl, λ_{exc} = 300 nm.

5. Conclusions

In this paper we have reported the development of a novel trimetallic hairpin complex for DNA recognition and luminescence sensing. The functionalized DTPA-bis(amide) framework linked to two square-planar Pt-tpy moieties *via* an ethynyl bridge proved to provide stable, emissive europium complexes with the advantage that the charge transfer band has been blue-shifted, compared to the analogues containing thiophenol linkers, away from the visible region of europium emission, allowing the strong europium signal to be detected. The heterometallic complex **1** showed the ability to bind DNA by bis-intercalating its Pt-tpy units, leading to stiffening of calf thymus DNA (typical of intercalators). The complex shows characteristic europium luminescence which is enhanced by three-fold upon interaction with ctDNA. The sensitisation takes place *via* the terpyridine moiety which intercalates to DNA but not from the charge transfer MLCT band. Furthermore, it appears the role of the Pt-tpy unit bis-intercalation (and the spatial constraints it confers) in positioning the europium complex close to DNA together with

effect on the charge transfer competing quenching pathways are important in the europium signal enhancement. Previously reported examples of lanthanide complexes attached to DNA intercalators most commonly show a *decrease* of lanthanide luminescence upon DNA interaction [46-49], with the exceptions being two DOTA macrocycle complexes, one with three naphthalene and one tetraazatriphenylene sensitiser (which likely intercalates) and the other with a bis-4- aminobenzamidine which likely binds in the minor groove. [50-51]. The three-fold *increase* in europium emission seen when our system binds to DNA is interestingly of a very similar magnitude to the effect in both of those systems. The results reported in this paper thus highlight that the design of heterometallic bis-intercalator complexes for DNA recognition are an effective approach for responsive sensitisation of a lanthanide luminescence signal.

Acknowledgements

This work was supported by the EU DNAREC Marie Curie Training Site (MEST-CT-2005-020842, L.S.) and E.D.G acknowledges support from DSTL. Some of the spectrometers used in this research were obtained, through Birmingham Science City: Innovative Uses for Advanced Materials in the Modern World (West Midlands Centre for Advanced Materials Project 2), with support from Advantage West Midlands (AWM) and partial funding by the European Regional Development Fund (ERDF).

References

[1]. Saeed HK, Sreedharan S, Jarman PJ, Archer SA, Fairbanks SD, Foxon SP, Auty AJ, Chekulaev D, Keane T, Meijer AJHM, Weinstein JA, Smythe CGW, de la Serna JB, Thomas JA (2020) Making the right link to theranostics: the photophysical and biological properties of dinuclear Ru-II-Re-I dppz complexes depend on their tether. J. Am. Chem. Soc. 142 (2):1101-1111. doi:10.1021/jacs.9b12564.

[2]. Caballero AB, Cardo L, Claire S, Craig JS, Hodges NJ, Vladyka A, Albrecht T, Rochford LA, Pikramenou Z, Hannon MJ (2019) Assisted delivery of anti-tumour platinum drugs using DNA-coiling gold nanoparticles bearing lumophores and intercalators: towards a new generation of multimodal nanocarriers with enhanced action. Chem. Sci. 10 (40):9244-9256. doi:10.1039/c9sc02640a.

[3]. Chan AK-W, Yam VW-W (2018) Precise modulation of molecular building blocks from tweezers to rectangles for recognition and stimuli-responsive processes. Acc. Chem.Res. 51 (12):3041-3051. doi:10.1021/acs.accounts.8b00339.

[4]. Pages BJ, Garbutcheon-Singh KB, Aldrich-Wright JR (2017) Platinum intercalators of dna as anticancer agents. Eur. J. Inorg. Chem. (12):1613-1624. doi:10.1002/ejic.201601204.

[5]. Gill MR, Derrat H, Smythe CGW, Battaglia G, Thomas JA (2011) Ruthenium(II) metallo-intercalators: DNA imaging and cytotoxicity. Chembiochem 12 (6):877-880. doi:10.1002/cbic.201000782.

[6]. Barraga F, Lopez-Senin P, Salassa L, Betanzos-Lara S, Habtemariam A, Moreno V, Sadler PJ, Marchan V (2011) Photocontrolled DNA binding of a receptor-targeted organometallic ruthenium(II) complex. J. Am. Chem. Soc.:110728093104028-110728093104028. doi:10.1021/ja205235m.

[7]. Ducani C, Leczkowska A, Hodges NJ, Hannon MJ (2010) Noncovalent DNA-binding metallo-supramolecular cylinders prevent DNA transactions in vitro. Angew. Chem. Inter. Ed. 49 (47):8942-8945. doi:10.1002/anie.201004471.

[8]. Turro C, Bossmann SH, Jenkins Y, Barton JK, Turro NJ (1995) Proton-transfer quenching of the mlct excited-state of ru(phen)$_2$dppz^{2+} in homogeneous solution and bound to dna. J Am Chem Soc 117 (35):9026-9032. doi:DOI 10.1021/ja00140a020.

[9]. Glasson CRK, Meehan GV, Clegg JK, Lindoy LF, Smith JA, Keene FR, Motti C (2008) Microwave Synthesis of a Rare [Ru2L3]4+ Triple helicate and its interaction with DNA. Chem. Eur. J. 14 (34):10535-10538. doi:10.1002/chem.200801790.

[10]. Hannon MJ (2007) Supramolecular DNA recognition. Chem. Soc. Rev. 36 (2):280-295. doi:10.1039/B606046N.

[11]. Galindo MA, Olea D, Romero MA, Gómez J, del Castillo P, Hannon MJ, Rodger A, Zamora F, Navarro JAR (2007) Design and non-covalent DNA binding of platinum(II) metallacalix[4]arenes. Che. Eur. J. 13 (18):5075-5081. doi:10.1002/chem.200601581.

[12]. Xu Y, McSally J, Andricioaei I, Al-Hashimi HM (2018) Modulation of Hoogsteen dynamics on DNA recognition. Nat. Commun. 9. doi:ARTN 1473

10.1038/s41467-018-03516-1.

[13]. Saeed HK, Saeed IQ, Buurma NJ, Thomas JA (2017) The structure of linkers affects the dna binding properties of tethered dinuclear ruthenium(ii) metallo-intercalators. Chem. Eur J 23 (23):5467-5477. doi:10.1002/chem.201605750.

[14]. Anderson CM, Taylor IR, Tibbetts MF, Philpott J, Hu YF, Tanski JM (2012) Hetero-multinuclear ruthenium(iii)/platinum(ii) complexes that potentially exhibit both antimetastatic and antineoplastic properties. Inorg. Chem. 51 (23):12917-12924. doi:10.1021/ic301981s.

[15]. Massai L, Fernandez-Gallardo J, Guerri A, Arcangeli A, Pillozzi S, Contel M, Messori L (2015) Design, synthesis and characterisation of new chimeric ruthenium(II)-gold(I) complexes as improved cytotoxic agents. Dalton Trans. 44 (24):11067-11076. doi:10.1039/c5dt01614b.

[16]. Bertrand B, Citta A, Franken IL, Picquet M, Folda A, Scalcon V, Rigobello MP, Le Gendre P, Casini A, Bodio E (2015) Gold(I) NHC-based homo- and heterobimetallic complexes: synthesis, characterization and evaluation as potential anticancer agents. J. Biol. Inorg. Chem. 20 (6):1005-1020. doi:10.1007/s00775-015-1283-1.

[17]. Wenzel M, Bigaeva E, Richard P, Le Gendre P, Picquet M, Casini A, Bodio E (2014) New heteronuclear gold(I)-platinum(II) complexes with cytotoxic properties: Are two metals better than one? J. Inorg. Biochem. 141:10-16. doi:10.1016/j.jinorgbio.2014.07.011.

[18]. Suntharalingam K, White AJP, Vilar R (2010) Two Metals Are Better than One: Investigations on the interactions between dinuclear metal complexes and quadruplex dna. Inorg. Chem. 49 (18):8371-8380. doi:10.1021/ic100884p.

[19]. Wheate NJ, Brodie CR, Collins JG, Kemp S, Aldrich-Wright JR (2007) DNA intercalators in cancer therapy: organic and inorganic drugs and their spectroscopic

tools of analysis. Mini-Reviews in Medicinal Chemistry 7:627. doi:https://doi.org/10.2174/138955707780859413.

[20]. Glover PB, Ashton PR, Childs LJ, Rodger A, Kercher M, Williams RM, De Cola L, Pikramenou Z (2003) Hairpin-shaped heterometallic luminescent lanthanide complexes for DNA intercalative recognition. J. Am. Chem. Soc. 125 (33):9918-9919. doi:10.1021/ja029886s.

[21]. Lewis DJ, Pikramenou Z (2014) Lanthanide-coated gold nanoparticles for biomedical applications. Coord. Chem. Rev. 273:213-225. doi:10.1016/j.ccr.2014.03.019.

[22]. Davies A, Lewis DJ, Watson SP, Thomas SG, Pikramenou Z (2012) pH-controlled delivery of luminescent europium coated nanoparticles into platelets. Proc Nat. Acad. Sci. USA 109 (6):1862-1867. doi:10.1073/pnas.1112132109.

[23]. Lewis DJ, Glover PB, Solomons MC, Pikramenou Z (2011) Purely Heterometallic Lanthanide(III) Macrocycles through Controlled Assembly of Disulfide Bonds for Dual Color Emission. J. Am. Chem. Soc. 133 (4):1033-1043. doi:10.1021/ja109157g.

[24]. Senechal-David K, Pope SJA, Quinn S, Faulkner S, Gunnlaugsson T (2006) Sensitized near-infrared lanthanide luminescence from Nd(III)- and Yb(III)-based cyclen-ruthenium coordination conjugates. Inorg. Chem. 45 (25):10040-10042. doi:Doi 10.1021/Ic061706i.

[25]. Castano-Briones MM, Bassett AP, Meason LL, Ashton PR, Pikramenou Z (2004) Controlled assembly of luminescent racks based on heteroleptic dinuclear lanthanide complexes. Chem. Commun. (024):2832-2833.

[26]. Zou TT, Liu J, Lum CT, Ma CS, Chan RCT, Lok CN, Kwok WM, Che CM (2014) Luminescent Cyclometalated platinum(ii) complex forms emissive intercalating adducts with double-stranded dna and rna: differential emissions and anticancer activities. Angew. Chem. Int. Edit. 53 (38):10119-10123. doi:10.1002/anie.201405384.

[27]. McGuire Jr R, McGuire MC, McMillin DR (2010) Platinum(II) polypyridines: A tale of two axes. Coord. Chem Rev 254 (21-22):2574-2583. doi:10.1016/j.ccr.2010.04.013.

[28]. Muro ML, Rachford AA, Wang XH, Castellano FN (2010) Platinum(II) acetylide photophysics. In: Lees AJ (ed) Top Organometal Chem, vol 29. Topics in Organometallic Chemistry. Springer-Verlag Berlin, Berlin, pp 159-191. doi:10.1007/3418_2009_1.

[29]. Sanchez-Cano C, Hannon MJ (2009) Cytotoxicity, cellular localisation and biomolecular interaction of non-covalent metallo-intercalators with appended sex hormone steroid vectors. Dalton Trans. (48):10765-10773. doi:10.1039/b912711a.

[30]. Williams JAG (2007) Photochemistry and photophysics of coordination compounds: Platinum. In: Top. Curr. Chem., vol 281. Topics in Current Chemistry. Springer-Verlag Berlin, Berlin, pp 205-268. doi:10.1007/128_2007_134.

[31]. Castellano FN, Pomestchenko IE, Shikhova E, Hua F, Muro ML, Rajapakse N (2006) Photophysics in bipyridyl and terpyridyl platinum(II) acetylides. Coord. Chem. Rev. 250 (13-14):1819-1828. doi:10.1016/j.ccr.2006.03.007.

[32]. Ma DL, Shum TYT, Zhang FY, Che CM, Yang MS (2005) Water soluble luminescent platinum terpyridine complexes with glycosylated acetylide and arylacetylide ligands: photoluminescent properties and cytotoxicities. Chem. Commun. (37):4675-4677. doi:10.1039/b507114c.

[33]. Wong KMC, Tang WS, Chu BWK, Zhu NY, Yam VWW (2004) Synthesis, photophysical properties, and biomolecular labeling studies of luminescent platinum(II)-terpyridyl alkynyl complexes. Organometallics 23 (14):3459-3465.

[34]. Wadas TJ, Lachicotte RJ, Eisenberg R (2003) Synthesis and characterization of platinum diimine bis(acetylide) complexes containing easily derivatizable aryl acetylide ligands. Inorg Chem 42 (12):3772-3778. doi:10.1021/ic0263084.

[35]. McMillin DR, Moore JJ (2002) Luminescence that lasts from Pt(trpy)Cl+ derivatives (trpy=2,2';6',2''-terpyridine). Coord. Chem. Rev. 229 (1-2):113-121. doi:10.1016/s0010-8545(02)00041-3.

[36]. Annibale G, Bergamini P, Bertolasi V, Bortoluzzi M, Cattabriga M, Pitteri B (2007) The relative coordinating ability of some weak O-donor anions and water towards the $[Pt(terpy)]^{2+}$ (terpy=2,2': 6',2 ''-terpyridine) center - X-ray crystal structures of $[Pt(terpy)(H_2O)](CF_3SO_3)_2$ and $[Pt\text{-}2(mu\text{-}OH)(terpy)_2](PF_6)_2(CF_3SO_3)$. Eur J Inorg Chem (36):5743-5751. doi:10.1002/ejic.200700777.

[37]. Yam VWW, Tang RPL, Wong KMC, Cheung KK (2001) Synthesis, Luminescence, electrochemistry, and ion-binding studies of platinum(ii) terpyridyl acetylide complexes. Organometallics 20 (22):4476-4482.

[38]. Chan WK, Ho CM, Wong MK, Che CM (2006) Oxidative amide synthesis and N-terminal alpha-amino group ligation of peptides in aqueous medium. J. Am. Chem. Soc. 128 (46):14796-14797. doi:10.1021/ja064479s.

[39]. Pappenfus TM, Burney JR, McGee KA, Lee GGW, Jarvis LR, Ekerholm DP, Farah M, Smith LI, Hinkle LM, Mann KR (2010) Alternative syntheses and reactivity of platinum(II) terpyridyl acetonitrile complexes. Inorg. Chim. Acta 363 (13):3214-3221. doi:10.1016/j.ica.2010.05.060 .

[40]. Lewis DJ, Day TM, MacPherson JV, Pikramenou Z (2006) Luminescent nanobeads: attachment of surface reactive Eu(III) complexes to gold nanoparticles. Chem. Commun. (13):1433-1435. doi:10.1039/b518091k.

[41]. Ruston LL, Robertson GM, Pikramenou Z (2010) Luminescence screening assays for the identification of sensitizers for lanthanides based on the controlled formation of ternary lanthanide complexes with dtpa-bisamide ligands. Chem. Asian J. 5 (3):571-580. doi:10.1002/asia.200900367.

[42]. Debroye E, Eliseeva SV, Laurent S, Vander Elst L, Petoud S, Muller RN, Parac-Vogt TN (2013) Lanthanide(III) complexes of diethylenetriaminepentaacetic acid (dtpa)-bisamide derivatives as potential agents for bimodal (optical/magnetic resonance) imaging. Eur. J. Inorg. Chem. (14):2629-2639. doi:10.1002/ejic.201300196.

[43]. Selvin PR (2002) Principles and biophysical applications of lanthanide-based probes. Annual Review of Biophysics and Biomolecular Structure 31:275-302. doi:10.1146/Annurev.Biophys.31.101101.140927.

[44]. Rodger A, Norden B (1997) Circular dichroism and linear dichroism. Oxford University Press.

[45]. Hannon MJ, Moreno V, Prieto MJ, Moldrheim E, Sletten E, Meistermann I, Isaac CJ, Sanders KJ, Rodger A (2001) Intramolecular DNA coiling mediated by a metallo-supramolecular cylinder Angew. Chem. Int. Ed. Engl. 40 (5):879-884. doi:10.1002/1521-3773(20010302)40:5.

[46] Bobba G, Kean SD, Parker D, Beeby A, Baker G. (2001) DNA binding studies of cationic lanthanide complexes bearing a phenanthridinium group J. Chem. Soc., Perkin Trans. 2 1738–1741 doi: 10.1039/ b303085g

[47] Bodi A, Estzer-Borbas, K., Bruce JI (2007) Near IR-emitting DNA-probes exploiting stepwise energy transfer processes Dalton Trans. 4352–4358. doi.org/10.1039/B708940F

[48] Nonat AM, Quinn SJ, Gunnlaugsson T (2009) Mixed f-d Coordination Complexes as Dual Visible- and Near-Infrared-Emitting Probes for Targeting DNA Inorg. Chem. 48, 4646–4648 DOI:10.1021/ic900422z

[49] Ancel L, Gateau C, Lebrun C, Delangle P (2013) DNA Sensing by a Eu-Binding Peptide Containing a Proflavine Unit Inorg. Chem. 52 552-554. dx.doi.org/10.1021/ic302456q

[50]. Bobba G., Bretonnière Y., Frias J-C, Parker D. (2003) Enantiopure lanthanide complexes incorporating a tetraazatriphenylene sensitiser and three naphthyl groups: exciton coupling, intramolecular energy transfer, efficient singlet oxygen formation and perturbation by DNA binding Org. Biomol. Chem. 1 1870–1872.

[51] Vázquez O, Sánchez MI, Mascareñas JL, Vázquez ME (2010) dsDNA-triggered energy transfer and lanthanide sensitization processes. Luminescent probing of specific A/T sequences Chem. Commun. 46 5518–5520.

Supplementary Material

A luminescent europium hairpin for DNA photosensing in the visible, based on trimetallic bis-intercalators

L. Scarpantonio, S. A. Cotton, E. del Giorgio, M.J. Hannon and Z. Pikramenou*

School of Chemistry, University of Birmingham, Edgbaston, B15 2TT, UK

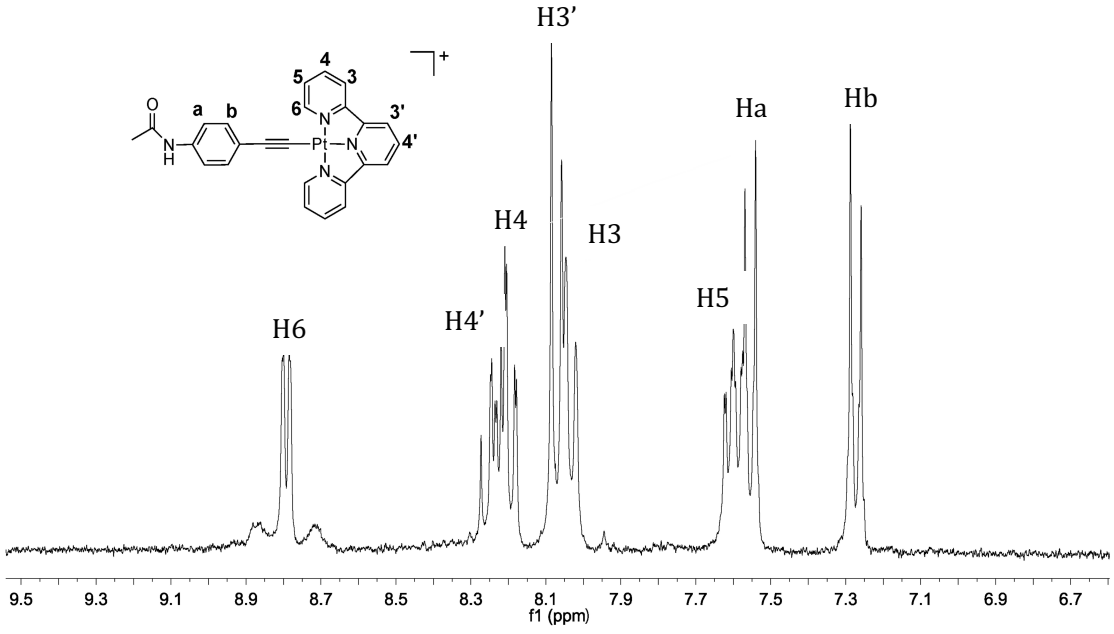

Figure S1 The aromatic region of the ^{1}H-NMR for **Pt-2b** complex in d_3-acetonitrile**.**

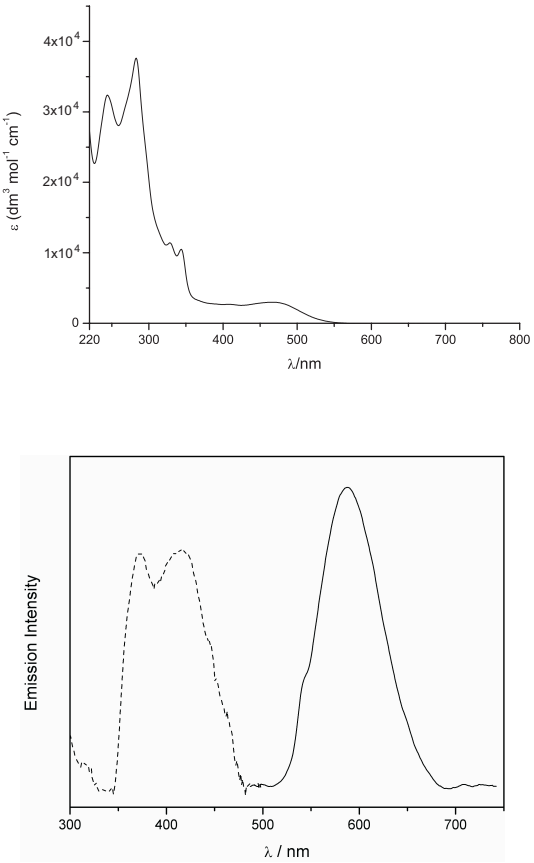

Figure S2. Absorption spectrum (top) and excitation and emission spectra of **2b** in degassed acetonitrile λ_{exc} = 430 nm, λ_{em} =585 nm.

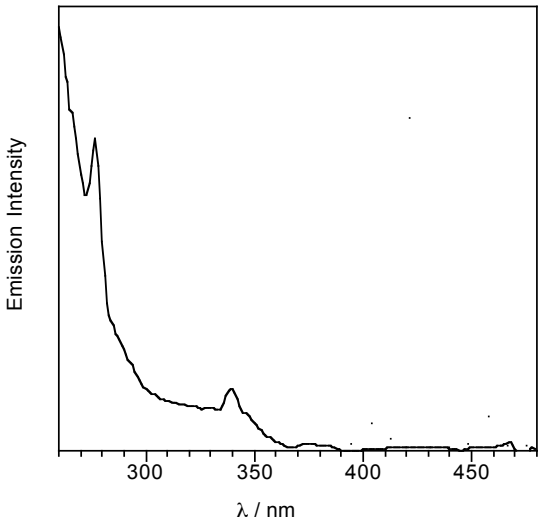

Figure S3 Excitation spectrum of **1** in methanol λem = 615 nm.

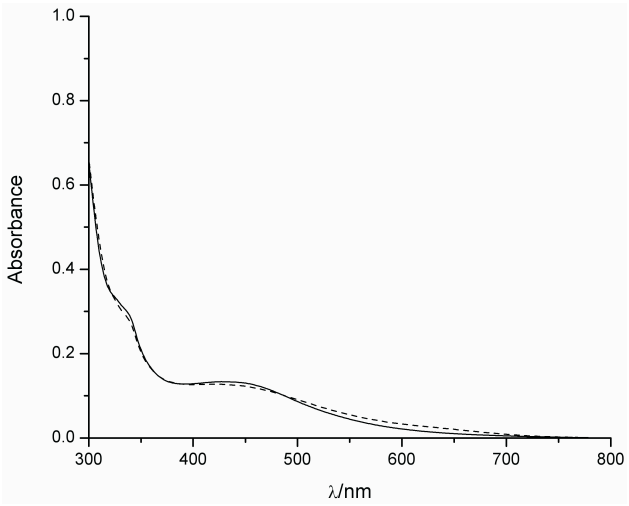

Figure S4 Absorption spectra of **2a** (solid line) and in presence of ctDNA (4:1 ctDNA:**2**). [ctDNA] = 40 □M in 10 mM HEPES and 10 mM NaCl.

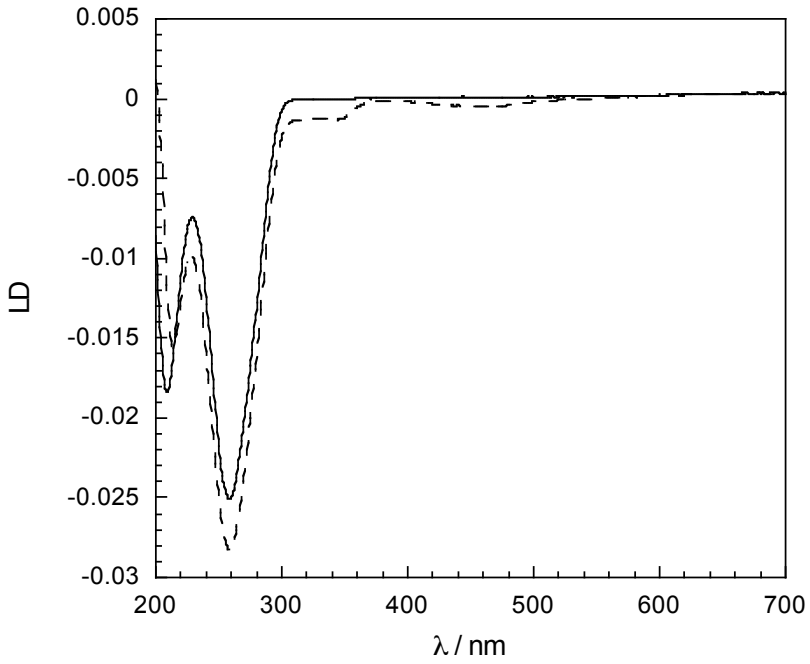

Figure S5. Linear dichroism spectra of ctDNA (solid line) and **2a** in presence of ctDNA (5:1 ctDNA:**2a**). [ctDNA] = 40 □M in 10 mM HEPES and 10 mM NaCl.

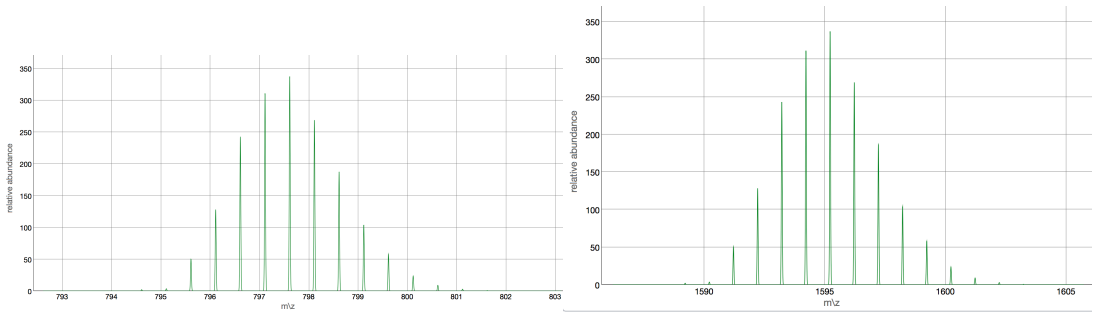

Figure S6. Theoretical isotope patterns of $[M-2(CH_3SO_3)]^{2+}$ and $[M-2(CH_3SO_3)]^{+}$